

## DARK MATTER CONTRACTION AND THE STELLAR CONTENT OF MASSIVE EARLY-TYPE GALAXIES: DISFAVORING “LIGHT” INITIAL MASS FUNCTIONS

M. W. AUGER<sup>1,†</sup>, T. TREU<sup>1,2</sup>, R. GAVAZZI<sup>3</sup>, A. S. BOLTON<sup>4</sup>, L. V. E. KOOPMANS<sup>5</sup>, P. J. MARSHALL<sup>6</sup>

*Draft version November 10, 2018*

### ABSTRACT

We use stellar dynamics, strong lensing, stellar population synthesis models, and weak lensing shear measurements to constrain the dark matter (DM) profile and stellar mass in a sample of 53 massive early-type galaxies. We explore three DM halo models (unperturbed Navarro Frenk & White [NFW] halos and the adiabatic contraction models of Blumenthal and Gnedin) and impose a model for the relationship between the stellar and virial mass (i.e., a relationship for the star-formation efficiency as a function of halo mass). We show that, given our model assumptions, the data clearly prefer a Salpeter-like initial mass function (IMF) over a lighter IMF (e.g., Chabrier or Kroupa), irrespective of the choice of DM halo. In addition, we find that the data prefer at most a moderate amount of adiabatic contraction (Blumenthal adiabatic contraction is strongly disfavored) and are only consistent with no adiabatic contraction (i.e., a NFW halo) if a mass-dependent IMF is assumed, in the sense of a more massive normalization of the IMF for more massive halos.

*Subject headings:* galaxies: elliptical and lenticular, cD — galaxies: halos — galaxies: structure — dark matter

### 1. INTRODUCTION

Numerical simulations of cold dark matter (CDM) halos predict density distributions with an inner logarithmic slope  $d\ln\rho/d\ln r = -1$  and a slope of  $d\ln\rho/d\ln r = -3$  at large radii (Navarro et al. 1996, 2010, hereafter NFW). However, the inclusion of baryons – and the dissipational processes associated with them – in galaxy formation simulations may significantly alter the central dark matter distribution. The DM may show an increased central density due to radiative dissipation from the baryons that depends on the mass of stars formed in the galaxy (e.g., the adiabatic contraction, or AC, models of Blumenthal et al. 1986; Gnedin et al. 2004, hereafter B86 and G04) or dynamical friction may counterbalance this effect (Abadi et al. 2009) and could result in cored profiles (e.g., El-Zant et al. 2004; Nipoti et al. 2004). The form of the CDM halo is critical for understanding the relative importance of baryonic and total mass in governing the structure of early-type galaxies (ETGs).

Strong lensing can measure masses to a few percent precision and is therefore a particularly powerful probe of this regime, by itself and in combination with other techniques (Treu 2010, and references therein). Studies have previously used strong and weak gravitational lensing (SL and WL) to constrain the distribution of DM for massive ETGs and found that the data are broadly and on average consistent with a NFW halo (e.g.,

Gavazzi et al. 2007). However, the SL and WL analysis alone cannot simultaneously probe the stellar mass  $M_*$  and central dark matter slope due to degeneracies (Lagattuta et al. 2009); additional information must be included to disentangle the contributions of stars and CDM to the central density distribution (similar to the disk-halo degeneracy for spiral galaxies). Schulz et al. (2009) have recently used WL and stellar velocity dispersions to investigate evidence for AC in SDSS ETGs. They find that the stellar velocity dispersions require more central mass than would be inferred from the stellar mass (assuming a Kroupa initial mass function, or IMF) and the central DM mass extrapolated from a NFW halo fit to the WL data. However, their findings are also consistent with no AC if a Salpeter IMF is assumed for the stellar component.

Jiang & Kochanek (2007) point out that the degeneracies between the central CDM slope and  $M_*$  can only be broken by using at least three mass probes. They use SL and dynamics to probe the central baryonic and CDM distribution of ETGs and include an ensemble measurement of the halo mass from WL data to find that AC models are favored over a NFW halo. However, Jiang & Kochanek (2007) assume a redshift-dependent but otherwise constant stellar mass-to-light ratio  $M_*/L$  for each of the galaxies, although the IMF (and therefore  $M_*/L$ ) may be non-universal (Treu et al. 2010). A full understanding of the central mass distribution of galaxies requires constraints on both the stellar and CDM components as a function of mass. Although this joint analysis is more complex and there are residual degeneracies, it provides a rare opportunity to constrain directly the IMF of distant massive ETGs where resolved stellar population diagnostics are not available (see, e.g., Cappellari et al. 2009; Bastian et al. 2010, and references therein).

In this Letter we present simultaneous constraints on  $M_*$  and the form of the central dark matter distribution for a sample of massive ETGs. We use SL, stellar dy-

<sup>1</sup> Department of Physics, University of California, Santa Barbara, CA 93106, USA

<sup>2</sup> Packard Fellow

<sup>3</sup> Institut d’Astrophysique de Paris, UMR7095 CNRS & Univ. Pierre et Marie Curie, 98bis Bvd Arago, F-75014 Paris, France

<sup>4</sup> Department of Physics and Astronomy, University of Utah, Salt Lake City, UT 84112

<sup>5</sup> Kapteyn Astronomical Institute, University of Groningen, P.O. Box 800, 9700AV Groningen, The Netherlands

<sup>6</sup> Kavli Institute for Particle Astrophysics and Cosmology, Stanford University, Stanford, CA 94305, USA

<sup>†</sup> mauger@physics.ucsb.edu

namics, stellar population synthesis (SPS) stellar mass estimates  $M_*^{\text{SPS}}$  given an IMF, and WL shear measurements to constrain a model for the relationship between stellar and virial mass. We allow for several different DM halo profiles and we fit for an IMF mismatch parameter relating  $M_*$  to  $M_*^{\text{SPS}}$  (Treu et al. 2010). The two main improvements over the analysis by Treu et al. (2010) are the inclusion of WL data and the adoption of more flexible models. We use a standard flat  $\Lambda$ CDM cosmology with  $\Omega_M = 0.3$  and  $h = 0.7$ .

## 2. THE DATA AND MODEL

Our sample is derived from the Sloan Lens ACS Survey (SLACS; Bolton et al. 2006; Gavazzi et al. 2007; Bolton et al. 2008; Auger et al. 2009), which consists of nearly 100 strong gravitational lensing galaxies. We exclude 6 galaxies which appear to be structurally different than the rest of the SLACS early-type lenses (Auger et al. 2010a). These systems are significant outliers from the otherwise very tight relation between effective radius, velocity dispersion, total central mass, and stellar mass; this is likely due to systematic errors in the stellar velocity dispersions of these systems (also see Jiang & Kochanek 2007). We therefore use a subsample of 53 ETGs that have well-determined central stellar velocity dispersions, SPS stellar masses assuming Chabrier (2003) and Salpeter (1955) IMFs, and central projected mass estimates from SL. We also use WL shear measurements for a subset of 44 lenses with deep ACS imaging. The details of how these data are derived can be found elsewhere (Gavazzi et al. 2007; Bolton et al. 2008; Auger et al. 2009, 2010a). We emphasize that the SLACS lens galaxies are indistinguishable from twin ETGs selected from SDSS to have the same velocity dispersion and redshift and can therefore be considered as representative of the overall population of massive ETGs (Treu et al. 2006, 2009; Auger et al. 2009, 2010a).

We model the lenses as two-component mass distributions consisting of stars and a CDM halo. Both components are modeled as spherical since our data do not constrain the halo flattening and our dynamical analysis is restricted to spherical Jeans modeling. Comparisons with non-spherical models shows that the most relevant quantities such as mass-density slope and total mass are relatively insensitive to this approximation (e.g., Barnabè et al. 2009).

The stars are modeled with the Hernquist (1990) profile and the scale radius is set by the rest-frame  $V$ -band effective radius,  $r_a = 0.551r_e$ ; our conclusions are unchanged if we adopt a Jaffe (1983) profile. We assume isotropic orbits, consistent with typical findings for massive ETGs (Barnabè et al. 2009). Mild radial anisotropy (Koopmans et al. 2009) only alters the inferred velocity dispersions by a few percent, i.e. an amount smaller than the errors, and therefore does not change our conclusions.

We investigate three different density profiles for the CDM halos. First, we consider the NFW profile with the concentration fixed by  $c(M_{\text{vir}}) \propto M_{\text{vir}}^{-0.094}$  following Macciò et al. (2008), neglecting intrinsic scatter for computational simplicity. We also modify the NFW halo to include AC using the prescriptions of B86 and G04, with the baryon fraction set by Equation 1 and the scale radius given by  $r_a$ ; these three profiles are the most widely adopted descriptions for CDM ha-

los (e.g., Jiang & Kochanek 2007; Schulz et al. 2009; Napolitano et al. 2010), and the NFW (B86) halo has the lowest (highest) central DM density.

We fix the relationship between stellar and virial mass to have the form suggested by Moster et al. (2010) (who use a Kroupa IMF) based upon abundance matching techniques. We assume

$$M_* \equiv M_*^{\text{SPS}} = M_{*,0} \frac{(M_{\text{vir}}/M_{\text{vir},0})^{\gamma_1}}{\left[1 + (M_{\text{vir}}/M_{\text{vir},0})^\beta\right]^{(\gamma_1 - \gamma_2)/\beta}} \quad (1)$$

where  $M_*^{\text{SPS}}$  is the stellar mass inferred from the SPS models assuming a Salpeter IMF,  $\gamma_1 = 7.17$ ,  $\gamma_2 = 0.201$ , and  $\beta = 0.557$  and we fit for  $M_{*,0}$  and  $M_{\text{vir},0}$ . We note that our results are qualitatively the same if we use different values for  $\gamma_1$ ,  $\gamma_2$ , and  $\beta$  (e.g., from Dutton et al. 2010), although the goodness-of-fit changes; we will explicitly fit for these parameters in a future paper to ascertain the extent to which one model prefers a given set of parameters over another.

We also allow for an offset between the model stellar mass and the SPS stellar mass, equivalent to a mass-dependent IMF (referred to as the ‘Free’ IMF model). The offset has the form

$$\log \frac{M_*^{\text{SPS}}}{M_*} = -\eta \log \frac{M_*}{10^{11} M_\odot} - \log \alpha, \quad (2)$$

where  $\alpha$  is equivalent to that introduced by Treu et al. (2010) and  $\eta$  is equivalent to the slope of Equation 5 in Treu et al. (2010). We adopt the  $M_*^{\text{SPS}}$  derived by Auger et al. (2009), although our results are robust with respect to changes in the SPS models and choice of priors (Treu et al. 2010) due to the relative simplicity of the older stellar populations of the SLACS ETGs. Uncertainties in SPS models of evolved galaxies (Conroy & Gunn 2010; Maraston et al. 2009) may lead to systematic offsets in  $M_*^{\text{SPS}}$  of order  $\sim 0.05$  dex (e.g., Treu et al. 2010).

We perform a Markov Chain Monte Carlo simulation to fit the models to the data; we propose  $M_{\text{vir}}$  for each lens and use Equation 1 (and 2 for the Free IMF model) to predict a stellar mass. These masses normalize the halo and bulge, and we use these profiles to predict the stellar kinematics, SL, and WL signals for each galaxy. We compare these quantities and the model stellar masses with the observed quantities on a galaxy-by-galaxy basis (i.e., we do not bin or average measurements, including the WL) to optimize the free model parameters and determine goodness-of-fit values.

## 3. RESULTS

The best-fit parameters and  $\chi^2$  for each model are listed in Table 1, and we show the best-fit mass distributions for a characteristic lens system ( $L_V = 10^{10.85} L_\odot$ ) in Figure 1. This illustrates that the low normalization of the Chabrier IMF requires a more massive CDM halo to increase the central projected mass and be consistent with the mass required by the SL data (this is true for the NFW *and* AC models). However, increasing the halo mass also increases the scale radius because the virial radius increases and the concentration becomes smaller (e.g., Macciò et al. 2008); therefore, the halo mass grows

at a faster rate than the projected dark matter mass inside the Einstein radius. The net effect is that very massive halos are needed to match the SL data if a Chabrier IMF is used (see Figure 2).

These massive halos cannot fit the SL masses *and* the WL shears (the inferred  $M_*$  values are also much higher than the measurements), and the data therefore clearly disfavor a Chabrier IMF (Table 1), consistent with the results from SL and dynamical constraints only (Treu et al. 2010). The G04 model is slightly preferred over the NFW halo for the Salpeter IMF while the B86 model is disfavored. The normalization and break point of the  $M_{\text{vir}}-M_*$  relation are consistent between the NFW and G04 model with a Salpeter IMF, and both are also consistent with the results from Moster et al. (2010) when the  $\sim 0.2$  dex offset between Kroupa and Salpeter IMFs is taken into account.

Figure 2 illustrates that the favored models require significantly higher star-formation efficiencies compared to the values of  $\approx 0.02 - 0.1$  (for a Chabrier IMF; double this for Salpeter) found for massive ETGs from galaxy-galaxy WL studies (e.g., Mandelbaum et al. 2006), which may point to a generic inadequacy of the family of models considered here. Interestingly, simulations of galaxy formation may require similarly high star-formation efficiencies to reproduce the observed isothermal central mass distributions of massive ETGs (Duffy et al. 2010) and suggest that the high efficiency may not be due to our simplifying assumptions.

The results for the free IMF model are somewhat more difficult to interpret due to the addition of two extra parameters; the fit is significantly improved compared to the fixed IMF models, as is expected when allowing for a more flexible model. The NFW model and G04 model fit the data equally well, but again the B86 model is disfavored. Note, however, that the form of the  $M_{\text{vir}}-M_*$  relation that we are using was derived assuming a constant IMF; allowing for a varying IMF would necessarily change the structural parameters  $\gamma_1, \gamma_2$ , and  $\beta$ . Nevertheless, the present model indicates that even the AC halos require the IMF to have a slight trend with mass in the sense that more massive galaxies require more Salpeter-like IMFs. The trend is stronger with the NFW halo (Figure 3) and is consistent with the relation found by Treu et al. (2010).

#### 4. DISCUSSION

There is a growing consensus that the fraction of DM at the center of massive ETGs increases with galaxy mass (Tortora et al. 2009; Napolitano et al. 2010; Graves & Faber 2010; Auger et al. 2010a). This increase could be due to a genuine increase in cold dark matter, perhaps as the result of AC mediated by the detailed accretion history of halos (e.g., Abadi et al. 2009; Lackner & Ostriker 2010). Alternatively, the trends may be the result of a mass-dependent IMF leading to more baryonic DM (in the form of low-mass stars or stellar remnants, depending on whether the IMF is bottom-heavy or top-heavy, respectively) in more massive galaxies (e.g., Treu et al. 2010), perhaps due to cosmic evolution of the IMF (van Dokkum et al. 2008) and a mass-dependent formation redshift for the stellar mass (e.g., Thomas et al. 2005; van der Wel et al. 2009).

##### 4.1. Ruling Out “Light” IMFs for Massive ETGs

We find that our sample of massive ETGs is inconsistent with a Chabrier IMF, even after allowing for strong CDM halo contraction and a mass-dependent IMF. Indeed, our data disfavor common “light” IMFs *generally*; the stellar mass derived assuming a Kroupa (2001) IMF is only  $\sim 0.06$  dex greater than  $M_*$  from a Chabrier IMF, which is not able to account for the  $\alpha$  values that we find (Table 1). We note that based on our data alone we cannot distinguish whether this is due to a higher abundance of low-mass stars (Salpeter-like), or of higher-mass stars and their neutron star and black hole remnants.

These results may appear to be inconsistent with those of Cappellari et al. (2006), who find that an IMF with a higher normalization than Kroupa (e.g., Salpeter) leads to stellar masses that are sometimes greater than the dynamical masses. However, we note that the tension is entirely due to fast-rotating or lower-mass galaxies, neither of which are typical of the SLACS lenses (e.g., Barnabè et al. 2009; Auger et al. 2010a); the SAURON data are consistent with our finding that massive ETGs do not have bottom-light IMFs (Cappellari et al. 2006).

##### 4.2. Adiabatic Contraction and a Varying IMF

The data also are opposed to strong adiabatic contraction, as modeled by B86. However, we cannot currently distinguish between a halo that has undergone mild AC and a NFW halo. This is partially due to imposing the form of the  $M_{\text{vir}}-M_*$  relation; if we use the Dutton et al. (2010) parameters for Equation 1 we find that for a fixed IMF the G04 model is strongly favored over the NFW model (and B86 is still disfavored), although we are again unable to distinguish between the two halos when the IMF is allowed to vary with mass.

Schulz et al. (2009) similarly found that a Kroupa IMF and adiabatically contracted halo or Salpeter IMF and no AC adequately fit the data, but they do not consider a mass-dependent IMF. Likewise, Jiang & Kochanek (2007) find that a Salpeter-like IMF and AC model is preferred (they do not directly compare their stellar masses with SPS model stellar masses, but their derived  $B$ -band  $M_*/L = 7.2 M_\odot/L_\odot$  is consistent with the  $M_*/L$  we find for the SLACS lenses assuming a Salpeter IMF, e.g., Auger et al. 2010a). Note, however, that they do not test for a mass-dependent IMF (their  $M_*/L$  is independent of mass).

##### 4.3. Beyond Structural Constraints

The structural decomposition into bulge+halo models is useful but may not be sufficient to fully understand how the IMF varies as a function of galaxy properties. We conclude by considering how non-structural constraints might be used to further discriminate between CDM and a non-universal IMF.

Napolitano et al. (2010) use stellar dynamics and SPS models to determine the DM fraction for a sample of ETGs and compare these with the predicted DM fractions from a suite of bulge+halo toy models. They find that a Kroupa IMF with AC or Salpeter IMF with no AC best represent their data, although they do not directly fit the models and do not allow for a mass-dependent star-formation efficiency. Nevertheless, they find an intriguing trend in which the IMF does not depend on

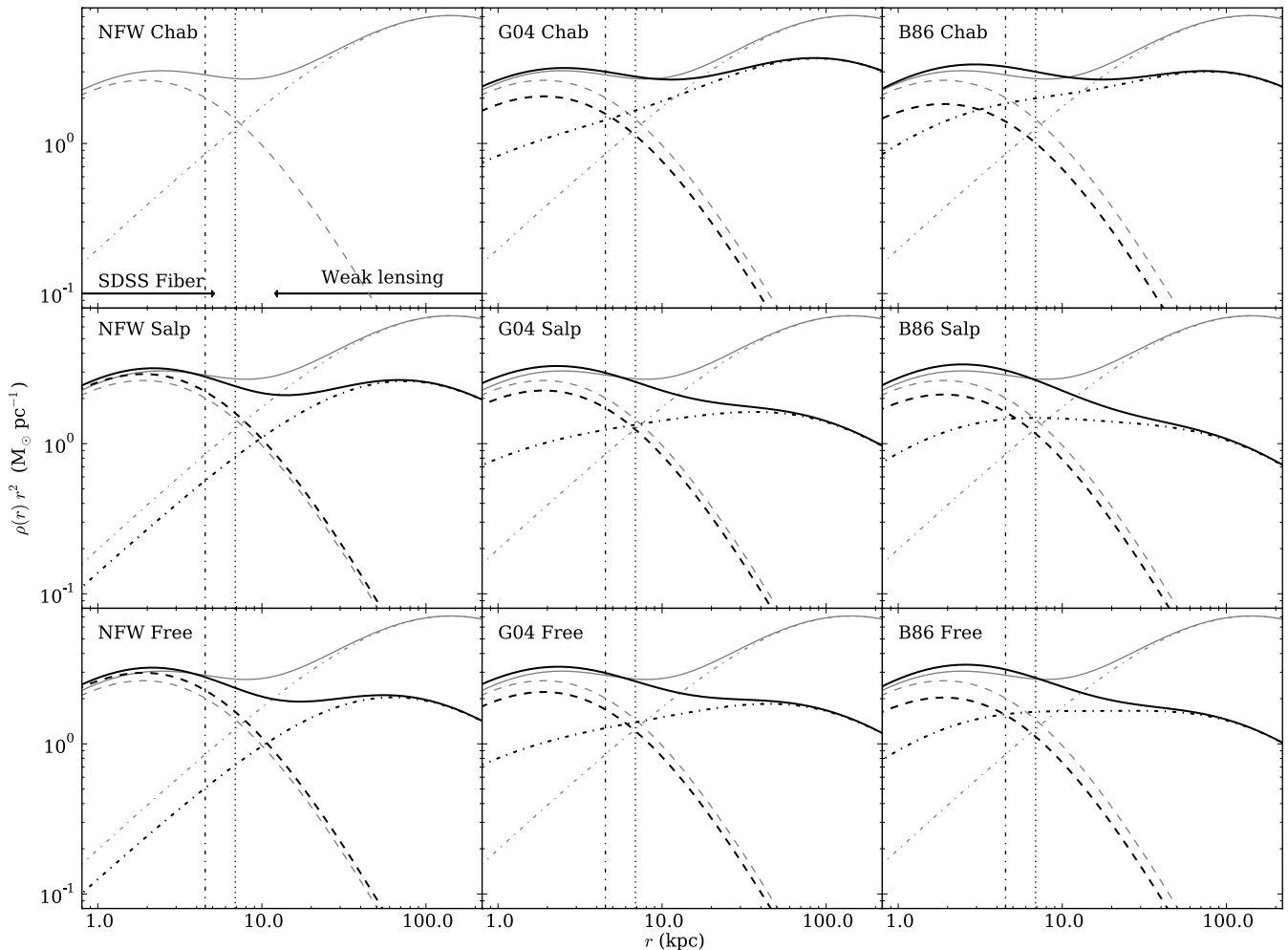


FIG. 1.— Bulge (dashed), halo (dot-dashed), and total mass (solid) profiles for each of the models investigated. The fiducial model, a NFW halo with Chabrier IMF, is shown in grey in each panel for comparison, and the vertical lines indicate the effective radius (dotted) and Einstein radius (dot-dashed); the radii probed by the stellar velocity dispersion and WL data are illustrated in the upper left panel. Note that the total mass profiles are approximately isothermal within the effective radius (e.g., Koopmans et al. 2006, 2009; Auger et al. 2010a). The Chabrier IMF models require large halo masses in order to provide enough projected mass within the Einstein radius to fit the SL data.

mass but may depend strongly on age in the sense that older galaxies have more Salpeter-like IMFs. As noted by Napolitano et al. (2010), this is the *opposite* trend than is expected from our relations. The cause of this discrepancy is unclear but may be related to how the samples are chosen. The SLACS lenses are at higher redshifts than the Napolitano et al. (2010) galaxies and are selected to have spectra that match old stellar templates; they would therefore only span ages between approximately 5 and 10 Gyr, for which the age-IMF trend is essentially flat.

Likewise, Graves & Faber (2010) use trends between mass and metallicity ( $[\text{Fe}/\text{H}]$ ,  $[\text{Mg}/\text{H}]$ , and  $[\text{Mg}/\text{Fe}]$ ) to investigate the role of the IMF on the central dark matter fraction. They show that the  $\alpha$ -enhancement of galaxies (e.g., the  $[\text{Mg}/\text{Fe}]$  ratio) is mass-dependent and could therefore signal a more top-heavy IMF in more massive galaxies such that the relative number of core-collapse supernovae increases in more massive galaxies. However, invoking more supernovae yields to super-abundant metallicities compared to the data, and another mechanism must therefore be posited in order to remove these metals (Graves & Faber 2010).

## 5. CONCLUSIONS

We have demonstrated that, given our standard assumptions, the IMF of massive ETGs cannot be “light”, even in the presence of significant adiabatic contraction. Furthermore, the IMF is only consistent with being universal if the central dark matter profile is mass dependent, as in the AC models presented here. It is clear that if one wants to preserve a light and universal IMF one has to abandon standard assumptions about dark matter halos, like the NFW profile. However, there are two important caveats. First, better constraints on the star-formation efficiency must be obtained from the data in order to draw definitive conclusions about the role of a mass-dependent IMF relative to CDM halo contraction. Second, although our conclusions are robust with respect to a wide variety of changes in our assumptions, we have not exhausted *all* possible families of theoretical models.

We will address these caveats, quantify the relationship between the central dark matter profile and the IMF in more detail, and quantify the consequences of our various assumptions in a forthcoming paper (Auger et al. 2010b, in preparation).

TABLE 1  
BEST FITTING PARAMETERS AND GOODNESS OF FITS

Halo	IMF	$\log[M_{*,0} / M_{\odot}]$	$\log[M_{\text{vir},0} / M_{\odot}]$	$\eta$	$\log \alpha$	$\chi^2/\text{d.o.f.}$	$\langle \ln P \rangle$
NFW	Chab	$11.38 \pm 0.09$	$11.32 \pm 0.24$	...	...	2.68	-19.16
	Salp	$11.29 \pm 0.04$	$10.38 \pm 0.06$	...	...	1.18	266.54
	Free	$11.44 \pm 0.06$	$10.52 \pm 0.07$	$0.08 \pm 0.04$	$0.03 \pm 0.03$	1.04	284.16
G04	Chab	$10.97 \pm 0.04$	$10.11 \pm 0.11$	...	...	1.66	189.76
	Salp	$11.36 \pm 0.05$	$10.43 \pm 0.05$	...	...	1.12	268.98
	Free	$11.26 \pm 0.06$	$10.34 \pm 0.06$	$0.03 \pm 0.05$	$-0.08 \pm 0.02$	1.08	281.58
B86	Chab	$10.94 \pm 0.04$	$10.07 \pm 0.10$	...	...	1.42	228.43
	Salp	$11.47 \pm 0.06$	$10.54 \pm 0.06$	...	...	1.26	234.00
	Free	$11.25 \pm 0.06$	$10.33 \pm 0.07$	$0.01 \pm 0.05$	$-0.11 \pm 0.02$	1.13	269.05

NOTE. — The ‘Free’ IMF is from Equation 2; for  $\eta = 0$ ,  $\log \alpha = 0$  for a Salpeter IMF and  $\log \alpha \approx -0.25$  ( $\log \alpha \approx -0.2$ ) for a Chabrier (Kroupa) IMF. The  $\chi^2$  is given for a model with the mean parameters listed in the table, although the interpretation of  $\Delta\chi^2$  is difficult due to the large number of degrees of freedom;  $\langle \ln P \rangle$  is the mean of the natural log of the posterior probability. It is also difficult to directly interpret  $\Delta\langle \ln P \rangle$ , but values of several tens clearly indicate a strong preference for one model over another.

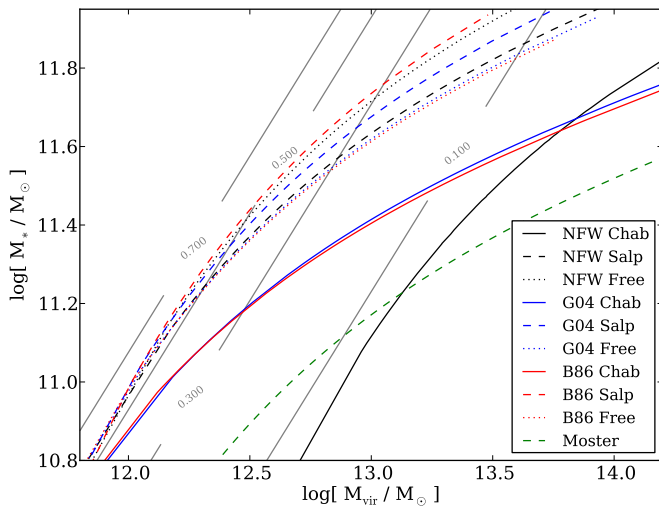


FIG. 2.— Best-fit  $M_{\text{vir}}-M_{*}$  relation for each of the bulge+halo models considered. Note that the models with a Chabrier IMF (solid lines) require substantially larger halo masses at fixed stellar mass in order to fit the SL data. The grey lines indicate contours of constant star-formation efficiency.

We thank the referee for his/her helpful comments, and Aaron Dutton and Matteo Barnabè for their suggestions. We acknowledge support from the NSF through CAREER award NSF-0642621, from the Packard Foundation through a Packard Fellowship to TT, and from NASA, through HST grants 11202, 10798, and 10494. RG is supported by the Centre National des Etudes Spatiales.

## REFERENCES

- Abadi, M. G., Navarro, J. F., Fardal, M., Babul, A., & Steinmetz, M. 2009, arXiv:0902.2477
- Auger, M. W., Treu, T., Bolton, A. S., Gavazzi, R., Koopmans, L. V. E., Marshall, P. J., Bundy, K., & Moustakas, L. A. 2009, ApJ, 705, 1099
- Auger, M. W., et al. 2010a, submitted to ApJ
- Auger, M. W., et al. 2010b, in preparation
- Barnabè, M., Czoske, O., Koopmans, L. V. E., Treu, T., Bolton, A. S., & Gavazzi, R. 2009, MNRAS, 399, 21
- Bastian, N., Covey, K. R., & Meyer, M. R. 2010, arXiv:1001.2965
- Blumenthal, G. R., Faber, S. M., Flores, R., & Primack, J. R. 1986, ApJ, 301, 27
- Bolton, A. S., Burles, S., Koopmans, L. V. E., Treu, T., & Moustakas, L. A. 2006, ApJ, 638, 703
- Bolton, A. S., Burles, S., Koopmans, L. V. E., Treu, T., Gavazzi, R., Moustakas, L. A., Wayth, R., & Schlegel, D. J. 2008, ApJ, 682, 964
- Cappellari, M., et al. 2006, MNRAS, 366, 1126
- Cappellari, M., et al. 2009, arXiv:0908.1904
- Chabrier, G. 2003, PASP, 115, 763
- Conroy, C., & Gunn, J. E. 2010, ApJ, 712, 833
- Duffy, A. R., Schaye, J., Kay, S. T., Vecchia, C. D., Battye, R. A., & Booth, C. M. 2010, MNRAS, 624
- Dutton, A. A., Conroy, C., van den Bosch, F. C., Prada, F., & More, S. 2010, arXiv:1004.4626
- El-Zant, A. A., Hoffman, Y., Primack, J., Combes, F., & Shlosman, I. 2004, ApJ, 607, L75
- Gavazzi, R., Treu, T., Rhodes, J. D., Koopmans, L. V. E., Bolton, A. S., Burles, S., Massey, R. J., & Moustakas, L. A. 2007, ApJ, 667, 176
- Gnedin, O. Y., Kravtsov, A. V., Klypin, A. A., & Nagai, D. 2004, ApJ, 616, 16
- Graves, G. J., & Faber, S. M. 2010, arXiv:1005.0014
- Hernquist, L. 1990, ApJ, 356, 359
- Jaffe, W. 1983, MNRAS, 202, 995
- Jiang, G., & Kochanek, C. S. 2007, ApJ, 671, 1568
- Koopmans, L. V. E., Treu, T., Bolton, A. S., Burles, S., & Moustakas, L. A. 2006, ApJ, 649, 599
- Koopmans, L. V. E., et al. 2009, ApJ, 703, L51
- Kroupa, P. 2001, MNRAS, 322, 231
- Lackner, C. N., & Ostriker, J. P. 2010, ApJ, 712, 88
- Lagattuta, D. J., et al. 2009, arXiv:0911.2236
- Macciò, A. V., Dutton, A. A., & van den Bosch, F. C. 2008, MNRAS, 391, 1940
- Mandelbaum, R., Seljak, U., Kauffmann, G., Hirata, C. M., & Brinkmann, J. 2006, MNRAS, 368, 715

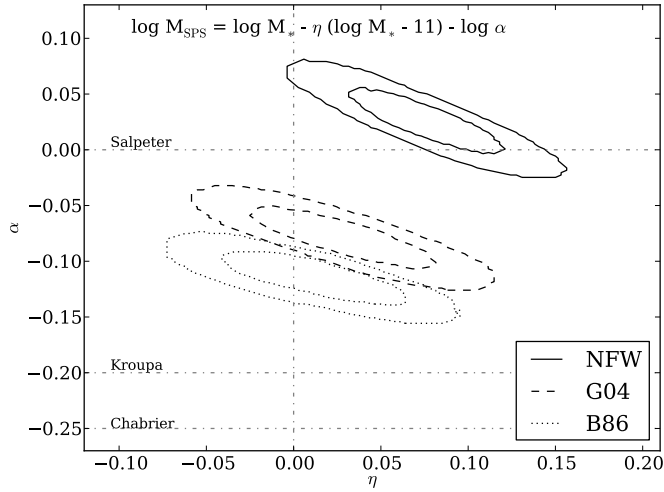


FIG. 3.— Constraints on the  $M_{\text{SPS}}$  mismatch model (Equation 2) assuming a NFW halo (solid contours), G04 halo (dashed contours), or B86 halo (dotted contours); the inner (outer) contour encloses 68% (95%) of the probability. The SPS masses were determined assuming the same IMF (Salpeter) for each galaxy and a non-zero  $\eta$  may therefore signal a mass-dependent IMF. The vertical line indicates a non-evolving IMF, and the horizontal lines denote the expected  $\alpha$  for common IMFs, as indicated.

- Maraston, C., Strömbäck, G., Thomas, D., Wake, D. A., & Nichol, R. C. 2009, *MNRAS*, 394, L107
- Moster, B. P., Somerville, R. S., Maulbetsch, C., van den Bosch, F. C., Macciò, A. V., Naab, T., & Oser, L. 2010, *ApJ*, 710, 903
- Napolitano, N. R., Romanowsky, A. J., & Tortora, C. 2010, *MNRAS*, 793
- Navarro, J. F., Frenk, C. S., & White, S. D. M. 1996, *ApJ*, 462, 563
- Navarro, J. F., et al. 2010, *MNRAS*, 402, 21
- Nipoti, C., Treu, T., Ciotti, L., & Stiavelli, M. 2004, *MNRAS*, 355, 1119
- Salpeter, E. E. 1955, *ApJ*, 121, 161
- Schulz, A. E., Mandelbaum, R., & Padmanabhan, N. 2009, arXiv:0911.2260
- Thomas, D., Maraston, C., Bender, R., & Mendes de Oliveira, C. 2005, *ApJ*, 621, 673
- Tortora, C., Napolitano, N. R., Romanowsky, A. J., Capaccioli, M., & Covone, G. 2009, *MNRAS*, 396, 1132
- Treu, T., Koopmans, L. V., Bolton, A. S., Burles, S., & Moustakas, L. A. 2006, *ApJ*, 640, 662
- Treu, T., Gavazzi, R., Gorecki, A., Marshall, P. J., Koopmans, L. V. E., Bolton, A. S., Moustakas, L. A., & Burles, S. 2009, *ApJ*, 690, 670
- Treu, T., Auger, M. W., Koopmans, L. V. E., Gavazzi, R., Marshall, P. J., & Bolton, A. S. 2010, *ApJ*, 709, 1195
- Treu, T. 2010, arXiv:1003.5567
- van der Wel, A., Bell, E. F., van den Bosch, F. C., Gallazzi, A., & Rix, H.-W. 2009, *ApJ*, 698, 1232
- van Dokkum, P. G., et al. 2008, *ApJ*, 677, L5